A Deep Learning Approach for Predicting Analyte Refractive Index of Open-Channel Plasmonic Sensor

Nazrul Islam
Department of Information and Communication Technology
Mawlana Bhashani Science and Technology University
Tangail-1902, Bangladesh

Imam Hossain Shibly
Department of Electrical and Electronic Engineering
University of Scholars, Dhaka 1213, Bangladesh

Md. Nahid Hasan
Department of Computer Science and Engineering
Dhaka International University, Dhaka-1212, Bangladesh

ABSTRACT
Open-channel plasmonic sensors utilize surface plasmon resonance (SPR) to detect minute changes in the refractive index (RI). This study presents a deep learning-based approach for predicting the analyte RI in plasmonic sensors. The work utilizing simulation data from a plasmonic sensor across a RI varies of 1.33 to 1.40. There are four deep learning methods such as artificial neural networks (ANNs), long short-term memory (LSTM) networks, gated recurrent units (GRUs), and convolutional neural networks (CNNs), is analyzed for their predictive capabilities. Among these methods, the ANN model demonstrates high performance, reaching an accuracy of 78.18%, with precision, recall, and F1-scores of 0.78, alongside minimal misclassification errors. On the other hand, the CNN and LSTM models exhibited moderate performance, each achieving 72.72% accuracy, while the GRU model lagged significantly with an accuracy of 41.81%. Analysis of training and test accuracies revealed stable ANN training accuracy at 90%, although test accuracy variations near 70% indicated potential overfitting. This work underscores the transformative potential of deep learning in advancing the design of plasmonic sensors and opening new avenues for biomedical sensing applications.

General Terms
Open-Channel, Plasmonic Sensor, Deep Learning.

Keywords
Plasmonic sensor, refractive index, wavelength sensitivity, Deep learning, Open-channel.

1. INTRODUCTION
Plasmonic sensors based on the SPR phenomenon and have attracted substantial attention in arenas such as biosensing [1], environmental monitoring [2], and chemical sensing [3]. Their acceptance stems from their highest sensitivity and rapid detection capabilities. The working process of these sensors is based on the interaction between light and free electrons on the metal surface. This interaction outcomes in a shift in the when analytes bind to the sensor surface [4]. The accurate prediction of the RI changes is crucial for refining the precision of these sensors. However, traditional models often face limitations. They struggle to handle complex, nonlinear relationships between sensor parameters and variations in RI. However, deep learning has emerged as an influential tool capable of capturing intricate patterns in large datasets. This makes it a promising approach for enhancing the predictive accuracy of plasmonic sensors [5]. By integrating deep neural networks (DNNs) and other advanced ML techniques, researchers aim to enhance prediction models. They also seek to optimize sensor performance.

Recent research [6], [7] have explored cutting-edge progresses in sensor design and the incorporation of ML. These efforts focus on optimizing sensor configurations for specific applications. The ML techniques are used to streamline and accelerate simulation workflows. It produces a feedforward multilayer perceptron-based ANN optimized with three hidden layers to prediction 12 optical parameters of silica based PCFs with maximum accuracy [8]. Moreover, the study utilizes ANNs to predict the output pulse shape parameters of a dissipative soliton resonance (DSR) fiber ring cavity laser. The ANN model precisely captures the complex nonlinear dynamics of fiber lasers, that is facilitating advanced system modeling [9]. Furthermore, the paper introduces an ultra-sensitive PCF-SPR sensor capable of detecting analyte RI with maximum sensitivity of 123,000 nm/RIU and highest prediction accuracy of 0.9987 [10]. Additionally, feedforward utilizes ANNs to accurately and efficiently compute the optical properties of solid-core PCF sensor [11].

Despite significant progresses in plasmonic sensing technologies and integration of deep learning methods for data analysis., Yet, there are few limitations predicting the analyte RI in open-channel plasmonic sensors using deep learning. Present models often goal conventional sensor designs or broader optical properties, leaving a gap in highly specialized, accurate, and real-time predictive tools tailored for open-channel outlines. This presents an opportunity to develop and evaluate deep learning integration and data profiles related with open-channel plasmonic sensors.

This work introduces a deep learning techniques for predicting the analyte RI of plasmonic sensor. This method enhances the accuracy of predicting RI variations. Deep learning is utilized to address challenges stemming from data scarcity and to expand the training dataset. This approach offers a capable solution for progressing the resent area of plasmonic sensing.

2. LITERATURE REVIEW
The study [12] introduces a dual-core gold-coated PCF-SPR biosensor optimized for analyte RI between 1.31 and 1.40. This is covered within wavelengths from 0.40 μm to 0.90 μm. By incorporating ML methods, particularly the random forest regressor, the sensor demonstrated high predictive accuracy. It also achieved a wavelength sensitivity of up to 9000 nm/RIU. It also achieving a maximum resolution of 1.11×10^{-5} RIU. Correspondingly, the paper [13] traveled various ML algorithms, including XGBoost, random forest, and PyTorch neural networks, to predict and optimize the sensitivity of a D-shaped PCF-SPR sensor. The XGBoost model achieved a high

prediction accuracy with an R^2 value of 99.64%. This is collective with the optimization algorithm, the sensor's high sensitivity rise from 4529.75 nm/RIU to 4814.14 nm/RIU.

According to [14], a gold-coated plasmonic sensor is accessible, tailored for the near-infrared detection of metabolic disorder biomarkers such as glucose and cholesterol. Leveraging a quasi-honeycomb structure and a deep neural network, the sensor achieved over 92% sensitivity and reduced computation time by 99.99%, enabling real-time, non-invasive monitoring. In paper [15] analyzes the use of ML method, particularly the gaussian process regressor (GPR), to optimize the figure of merit (FOM) for PCF-SPR sensors based on differences in wavelength and metal layer thickness. The GPR model demonstrated strong trend consistency and predictive accuracy, achieving FOM values of 6526.23 and 6356.98 at specific wavelengths across different datasets. These findings highlight the model's effectiveness in purifying sensor design before real time implementation.

The study [16] presents a PCF-SPR sensor enhanced with four nanowires with gold. This is achieved wavelength sensitivities ranging from 2000 to 18000 nm/RIU within the wavelength range 720–1280 nm. The authors accurately predicted confinement loss and sensitivity using ANN. This is achieved the mean squared errors as low as 0.002. It also shows the integration of ML in enhancing sensor performance. Moreover, in the paper [17] offerings a visible core PCF sensor enhanced with gold-based SPR. It is achieved a high wavelength sensitivity of 23,000 nm/RIU. It is also achieved FOM value of 287.50 RIU^{-1} for enhanced sensor performance. The RI range is between 1.33 and 1.41. Within this range, the sensor is effective at detecting a diverse range of substances. It covers cancer cells. Enhanced prediction accuracy is achieved through support vector regression.

The work presented in [18] highlighted the use of k-nearest neighbor regression (KNNR). This method was applied to predict loss features in a bent PCF-SPR sensor. The KNNR shows high performance across 1,180 samples. It is including straight and bent fibers in both x and y orders. It shows that KNNR not only outstrips ANN and linear least squares regression. It also suggests the advantage of instant usability without lengthy training. This highlights KNNR's potential. It serves as an effective alternative for optical sensor simulations. It also shows potential for real-time sensor investigation.

3. DEEP LEARNING MODEL IMPLEMENTATION

3.1 Dataset Details

In this research, the dataset was collected using a plasmonic sensor, as full information in [19]. It holds 1,902 data. The inputs are RI, wavelength (λ), confinement loss (α), and the real and imaginary components of the material. Moreover, the dataset includes the real (Re_{eff}) and imaginary (Im_{eff}) parts of the effective RI. The datasets are arranged into eight separate analyte RI intervals. The RI change between 1.33 and 1.40. This wide-ranging dataset provides a solid foundation for investigating the RI. It is a vital parameter in plasmonic sensor research.

3.2 System Configuration

The experiments were conducted using a deep neural network implemented using Python. This is leveraging the PyTorch framework. The system is used a high-performance workstation. It is configured with a quad-core Intel Core i7 processor at 2.6 GHz. This is also supported by 16 GB of 2400 MHz DDR4 RAM. The workstation is equipped with an NVIDIA GTX 960M GPU. It is featuring 4 GB of dedicated video memory for enhanced graphical processing. It is running on the Windows 10 operating system, the PyTorch framework. It also optimized to fully harness the GPU's computational power fully and effective algorithm implementation.

3.3 Evaluation Metric in Plasmonic Sensor

The feedforward neural network is used to predict the RI based on input parameters derived from plasmonic sensor data as shown Figure 1. The input layer consists of six features: Wavelength, Real, Imaginary, y-real, y-img, and confinement loss. The network incorporates four hidden layers with decreasing numbers of nodes: hidden layer 1 includes 128 nodes, hidden layer 2 has 64 nodes, hidden layer 3 contains 32 nodes, and hidden layer 4 comprises 16 nodes. Each hidden layer is densely connected to the previous layer, allowing for efficient processing and transformation of input features through nonlinear activation functions.

The output layer consists of eight nodes corresponding to discrete RI values varies between 1.33 and 1.40. This is enabling the network to predict the most probable RI value based on the provided input. ML evaluation metrics play a vital role in considering the function of plasmonic sensors. This is relied on SPR for high-sensitivity detection applications. Performance evaluation metrics such as accuracy, precision, F1-score, and recall enable researchers to quantitatively evaluate the performance of predictive models applied to plasmonic data. These metrics ensure robust validation. They also provide insights into the reliability and efficacy of ML algorithms in identifying subtle changes in sensor responses.

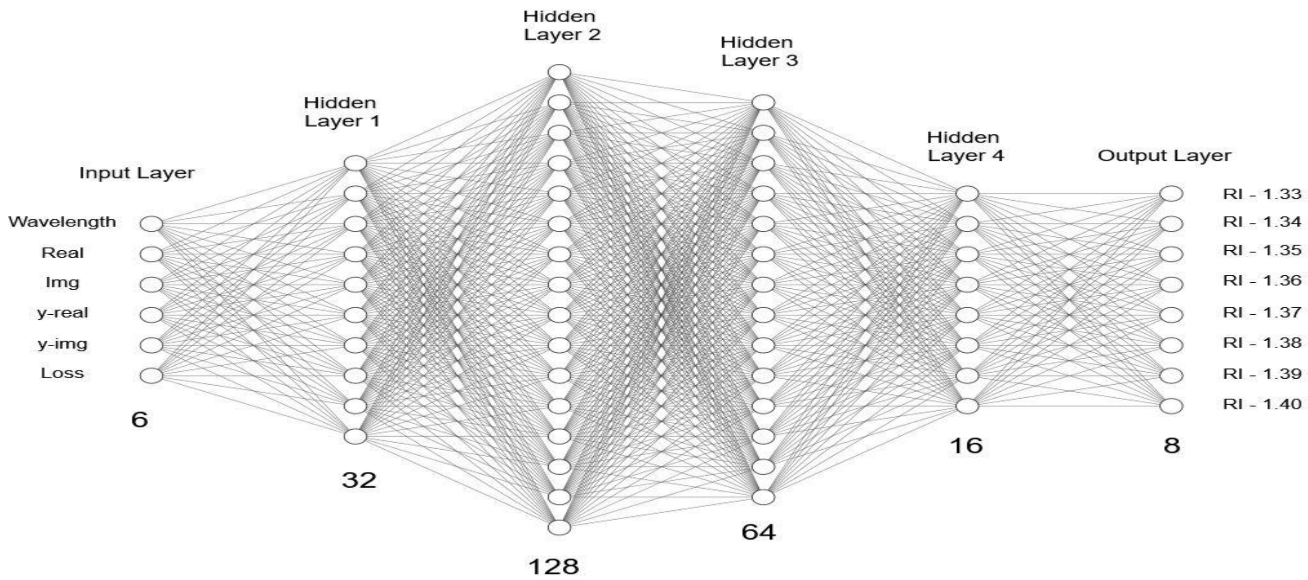

Fig. 1. Workflow of the Proposed Work

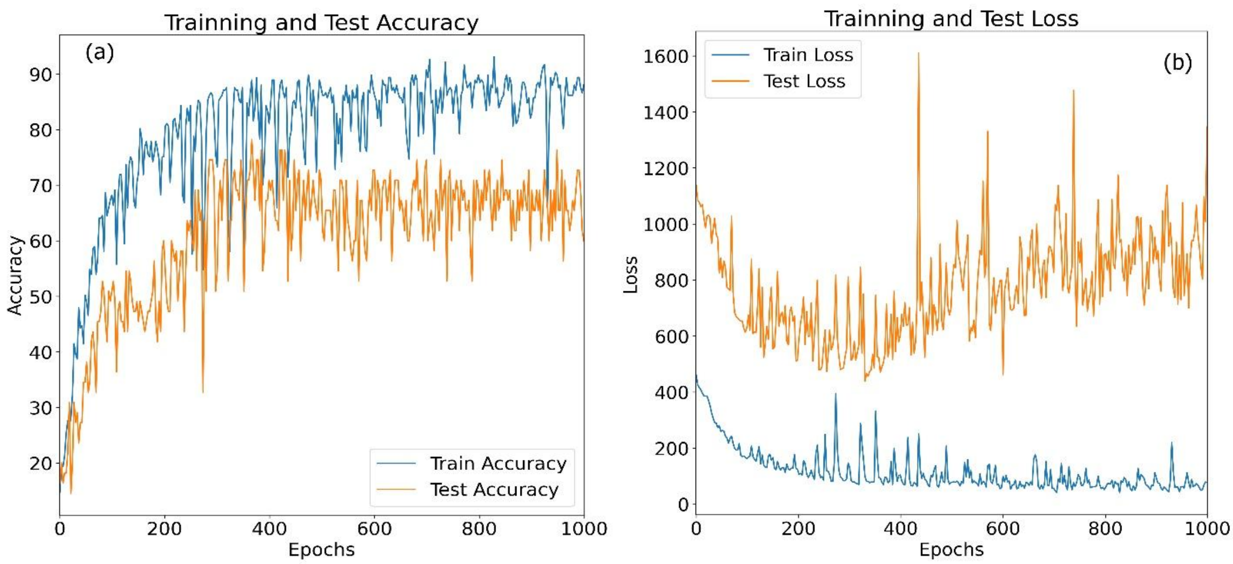

Fig. 2. (a) Training and Test accuracy of ANN (b) Train and Test Loss of ANN

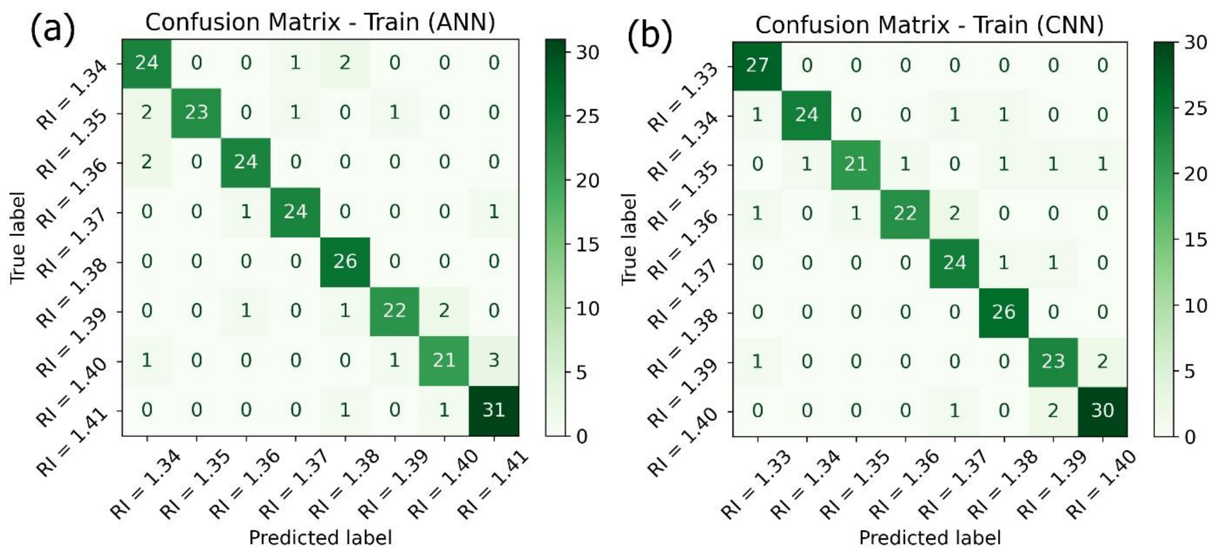

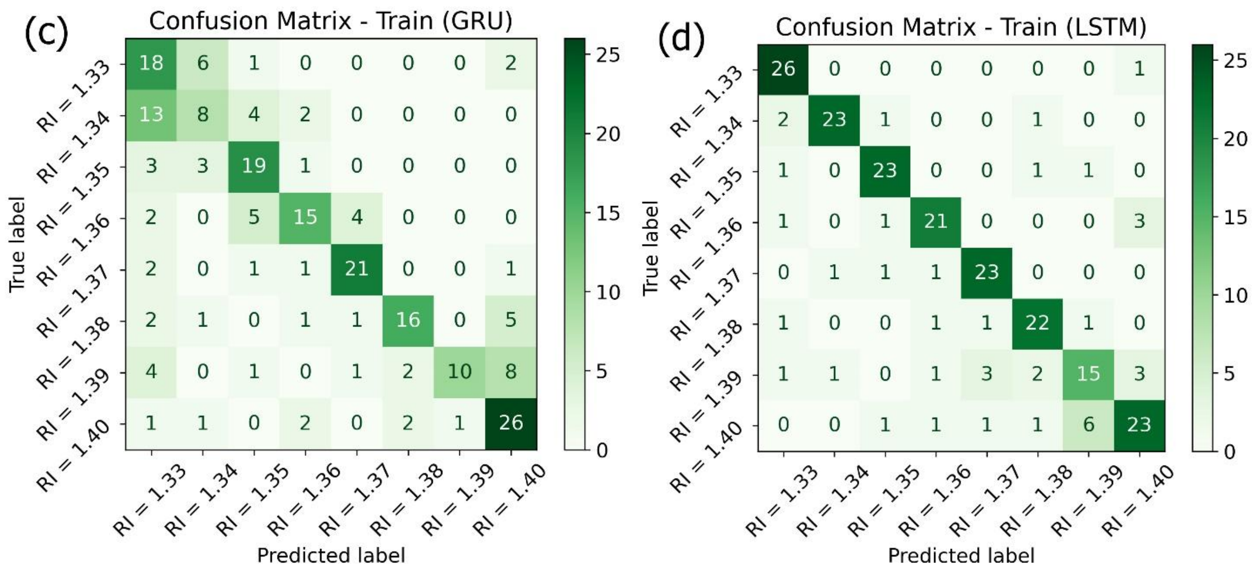

Fig. 3. Confusion matrix of (a) ANN, (b) CNN, (c) GRU, (d) LSTM

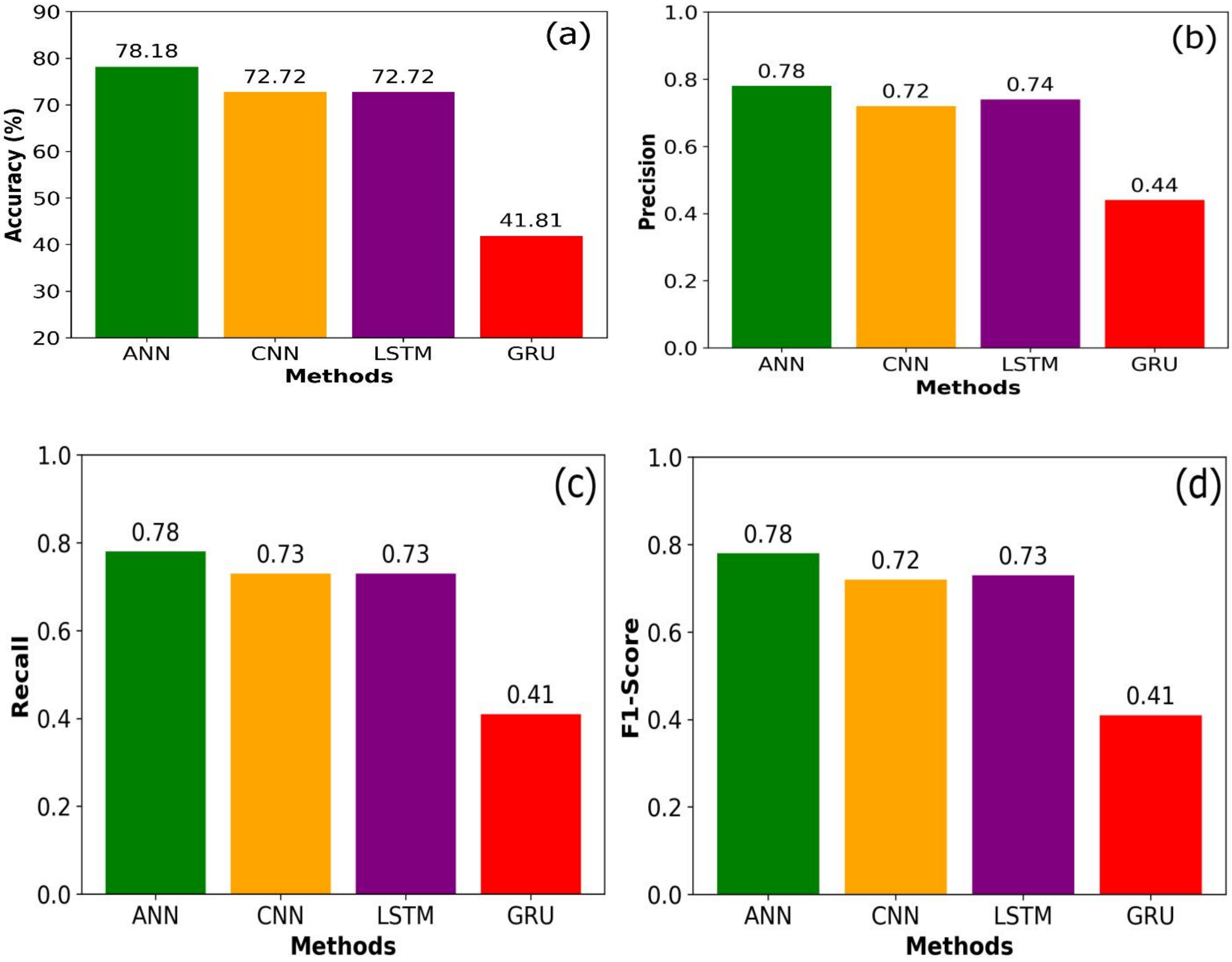

Fig. 4. Performance metrics with (a) accuracy, (b) precision, (c) recall, (d) F1-Score

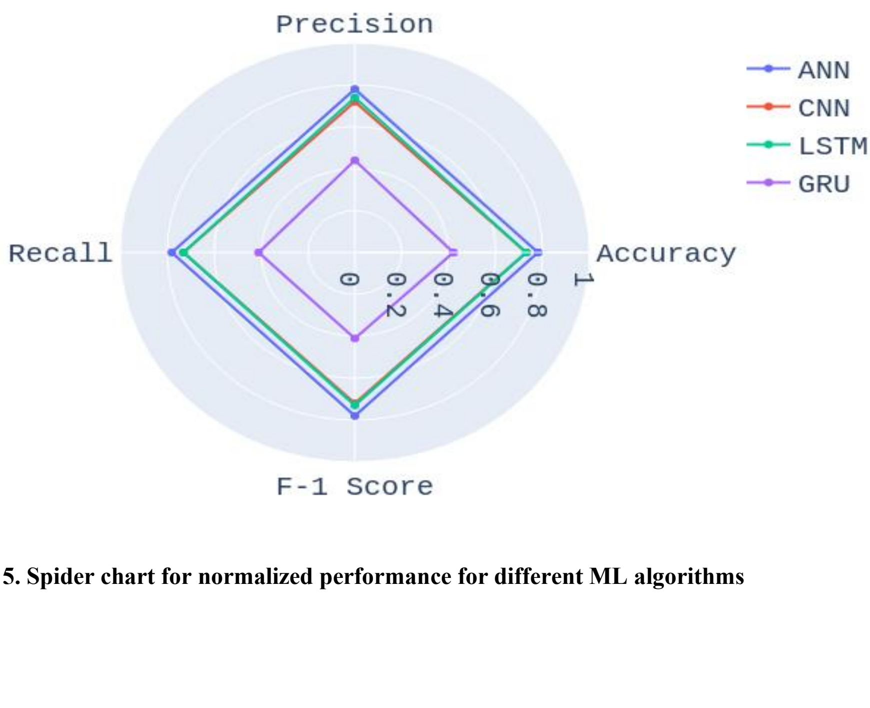

Fig. 5. Spider chart for normalized performance for different ML algorithms

4. RESULTS AND ANALYSIS

The deep learning model is analyzed during its training process by examining both training loss and test loss over 1000 epochs. It also provides insight into how well the model performs on both seen and unseen data. In Figure 2(a), the training loss is shown to decline steadily. It also indicates that the model is enlightening its performance on the data it was trained on. As the model learns from the training dataset, it becomes more adept at diminishing errors. Moreover, the training accuracy progresses and stabilizes at about 90%. This proposes that the model is successfully learning the training data. However, in Figure 2(b), the test loss remains higher and varies significantly, mainly after the first 400 epochs. This behavior points to the model stressed with the test data. It has not seen before, and shows a lack of reliability in its performance on this data.

The difference between the training accuracy and test accuracy proposes that the model is overfitting. Overfitting occurs when a model becomes too particular to the training data. The learning patterns that are detailed to the training set rather than generalizable patterns that would apply to new, unseen data. In this case, the model attains high accuracy on the training data in around 90%. Moreover, the test accuracy emphasized at only 70%. It indicates that the model's ability to simplify to new data is limited. This issue is additional recognized by the behavior of the test loss. It fails to drop in the same way the training loss does. Instead, the test loss remains classy. It also shows substantial variations beyond the 400^{th} epoch. This is a typical sign of overfitting. Furthermore, the model has learned the training data too well. It is failing to apply its learning effectively to the test data. These trends indicates that the model, while effective in learning from the training data. It does not exhibit reliable performance when applied to new data. It also indicates room for enhancement in its ability to generalize.

The confusion matrices for ANN are shown in Figure 3(a). It provides an in-depth view of their performance on the training dataset for analyte detection across the RI coverage of 1.33–1.40. The ANN model demonstrates high predictive accuracy. I also aligning most predictions closely with the actual RI values. For instance, the ANN correctly classifies RI = 1.41 in 31 cases, with only one misclassification. It also achieves 24 correct classifications for RI = 1.34, with minimal false positives or negatives. The low number of off-diagonal elements in the ANN confusion matrix underscores its robustness. This indicates strong performance across all RI classes.

Figure 3(b) illustrates the CNN model, which performs well but exhibits slightly higher misclassification rates compared to the ANN. For example, the CNN correctly predicts RI = 1.33 in 27 cases, though it struggles slightly with RI = 1.35 and RI = 1.39. These predictions are distributed across neighboring RI classes. This highlights a weaker generalization ability in the CNN compared to the ANN, especially for mid-range refractive indices such as 1.36–1.38. Overall, the outcomes indicates that the ANN outperforms the CNN in terms of predictive accuracy and consistency. The ANN model demonstrates clearer separability between actual and predicted classes. Moreover, the CNN exhibits a slightly higher prediction overlap.

Figure 3(c) illustrates the GRU model's performance in classifying RI values ranging from 1.33 to 1.40 during training. The model achieves an overall accuracy of approximately 75.57%. The highest classification accuracy observed for RI = 1.40 and RI = 1.37 that is indicating strong model confidence in these classes. However, significant misclassifications occur between neighboring RI values. This is particularly for RI = 1.34, which is frequently predicted as RI = 1.33 or RI = 1.35. This pattern highlights the model's difficulty in distinguishing between closely spaced RI values. This is a common challenge in fine-grained classification tasks. The results indicates that the GRU captures general trends. However, refinement or regression may better handle the continuous nature of RI data.

The Figure 3(d) for the LSTM model on the training data reveals a high overall classification accuracy in predicting RI values. This is most predictions concentrated along the diagonal and demonstrating correct classifications. The model exhibits influential performance for RI values of 1.33, 1.34, 1.35, 1.36, and 1.37. In these cases, misclassifications are minimal or non-existent. The confusion is more noticeable in the higher RI ranges (1.38 to 1.40), especially for RI = 1.39. It is sometimes misclassified as RI = 1.36, 1.37, or 1.40. Despite these minor confusions, the model demonstrates a clear ability to differentiate between closely spaced RI values. It outperforms the GRU model in terms of precision and consistency across all classes. This indicates that the LSTM model captures the sequential or temporal patterns in the data more effectively. This makes it well-suited for this classification task, which involves subtle numerical distinctions.

Figure 4(a-d) compares the function of four ML method using evaluation metrics: accuracy, recall, precision, and F1-score. Among the models, ANN consistently outstripped the others all metrics, achieving the highest accuracy of 78.18%, precision of 0.78, F1-score of 0.78, and recall of 0.78. The techniques CNN and LSTM showed comparable performance, with accuracy, recall, and F1-scores of 72.72% and approximately 0.73, respectively. However, GRU demonstrated significantly lower performance, achieving an accuracy of only 41.81%, with precision, F-1 score and recall values dropping to 0.44 or below. These results highlight ANN's superior ability to capture patterns in the dataset and generalize effectively. While CNN and LSTM performed reasonably well, they did not reach the same level of precision and recall as ANN. As reflected in its low metrics, GRU, being the least effective, struggled to provide consistent predictions. These findings align with the earlier confusion matrix analysis, confirming ANN as the most suitable algorithm for this SPR-PCF biosensor applications.

The radar chart shows in see Figure. 5, compares the performance of four neural network methods, such as ANN, CNN, LSTM, and GRU, across all evaluation metrics such as accuracy, recall, precision, and f-1 score. Comapre all the models, ANN consistently demonstrates the highest performance across all parameters, closely followed by CNN and LSTM, which show similar results. GRU, on the other hand, lags significantly behind the others in every category, indicating a comparatively weaker performance. This visualization effectively highlights the superior overall efficiency of ANN in this particular evaluation.

5. CONCLUSIONS

This study has highlighted the effectiveness of deep learning-based approaches for predicting the analyte RI in open-channel plasmonic sensor. The range of the RI is 1.33 to 1.40. Among the four ML method evaluated, the ANN model demonstrated superior performance. This is achieved the highest accuracy of 78.18% with precision, F1-scores, and recall of 0.78 each. In comparison, the CNN and LSTM models have shown moderate accuracies of 72.72%, while the GRU model has underperformed significantly, with an accuracy of 41.81%. The ANN model has consistently achieved a training accuracy of

90%. However, the test accuracy fluctuations near 70% have indicates potential overfitting. This study has established the ANN model as the most robust and reliable architecture for predicting RI. It also provides valuable numerical perceptions to guide future work. These outcomes highlight the transformative possible of deep learning techniques in plasmonic sensor design. They also offer hands-on insights for forward-moving biomedical sensing applications.

Future work will be expanding the RI range outside 1.33 to 1.40. This also include more numerous analyte features could be positive. It would also allow the plasmonic sensors to be functional in more wide-ranging analytical atmospheres.

6. REFERENCES

[1] Simone, G. 2024 "Trends of biosensing: plasmonics through miniaturization and quantum sensing," Critical Reviews in Analytical Chemistry, vol. 54, no. 7, pp. 2183–2208.

[2] Singh, K., Pombeiro, A. J., Garazade, I. M., Q. Sun, and Mohan, B., 2024. "Plasmon-enhanced fluorescence sensors for food and environmental samples monitoring," Microchemical Journal, p. 109888.

[3] Baz, A., Wekalao J., Mandela, N., and Patel, S. K., 2024 "Design and performance evaluation of machine learning-based terahertz metasurface chemical sensor, " IEEE Transactions on NanoBioscience.

[4] Philip, A. and Kumar, A. R., 2022. "The performance enhancement of surface plasmon resonance optical sensors using nanomaterials: A review," Coordination Chemistry Reviews, vol. 458, p. 214424.

[5] Li, M., He, X., Wu, C., Wang, L., Zhang, X., Gong, X., Zeng, X., and Huang, Y., 2024 "Deep learning enabled sers identification of gaseous molecules on flexible plasmonic mof nanowire films," ACS sensors, vol. 9, no. 2, pp. 979–987.

[6] Masson, J.-F., Biggins, J. S., and Ringe, E., 2023 "Machine learning for nanoplasmonics," Nature Nanotechnology, vol. 18, no. 2, pp. 111–123.

[7] Kaziz, S., Echouchene, F., and Gazzah, M. H., 2024 "Optimizing pcf-spr sensor design through taguchi approach, machine learning, and genetic algorithms" Scientific Reports, vol. 14, no. 1, p. 7837.

[8] Jabin, M. A. and Fok, M. P., 2022 "Prediction of 12 photonic crystal fiber optical properties using mlp in deep learning," IEEE Photonics Technology Letters, vol. 34, no. 7, pp. 391–394.

[9] Mezzi, F. Bahloul, Karar, A. S., Ghandour, R., and Salhi, M., 2023 "Predicting behavior of photonic crystal fiber lasers using artificial neural networks," Optics Communications, vol. 542, p. 129582.

[10] M. A. Mim, M. R. Khatun, M. M. Hossain, and W. Rahman, 2025 "Advanced pcf-spr biosensor design and performance optimization using machine learning techniques," Optik, p. 172391.

[11] Chugh, S., Gulistan, A., Ghosh, S., and Rahman, B., 2019 "Machine learning approach for computing optical properties of a photonic crystal fiber," Optics express, vol. 27, no. 25, pp. 36 414–36 425.

[12] Mim, M. A., Khatun, M. R., Hossain, M. M., and Rahman, W., 2025 "Advanced pcf-spr biosensor design and performance optimization using machine learning techniques," Optik, p. 172391.

[13] Y, Dogan, R., Katirci, and Erdogan, I., 2025 "Machine learning-based optimization for d-shaped pcf spr refractive index sensor," Optics Communications, vol. 575, p. 131304.

[14] Sharma, S., Das, S., Shieh, C.-S., M.-F, Horng, L., Tharani, Sharma, S., Sharma, P., Chakrabarti, P., and Rawal, Y. S., 2025 "Design and numerical analysis of a gold-coated photonic crystal fiber sensor for metabolic disorder detection with deep learning assistance," Plasmonics, pp. 1–11.

[15] Dwivedi, Y. S., Singh, R., Sharma, A. K., and Sharma , A. K., 2022 "Enhancing the performance of photonic sensor using machine-learning approach," IEEE Sensors Journal, vol. 23, no. 3, pp. 2320–2327.

[16] Ehyaee, A., Rahmati, A., Bosaghzadeh, A., and Olyaee , S., 2024 "Machine learning-enhanced surface plasmon resonance based photonic crystal fiber sensor" Optics Express, vol. 32, no. 8, pp. 13 369–13 383.

[17] Ali, Y. A. A., Rahman, A., Almawgani , A. H., Mollah , M. A., and Alabsi, B. A., 2025 "Internal sensing with exposed core fiber plasmonic sensor and machine-learning approach for ri prediction," Plasmonics, pp. 1–10.

[18] Kalyoncu, C., Yasli, A., and Ademgil, H., 2022 "Machine learning methods for estimating bent photonic crystal fiber based spr sensor properties," Heliyon, vol. 8, no. 11.

[19] Islam, N., Hasan, M. M. S., Shibly, I. H, M. Rashid B., Yousuf, M. A., Haider, F., Aoni, R. A., and Ahmed, R., 2024 "Plasmonic sensor using generative adversarial networks integration," Optics Express, vol. 32, no. 20, pp. 34 184–34 198.